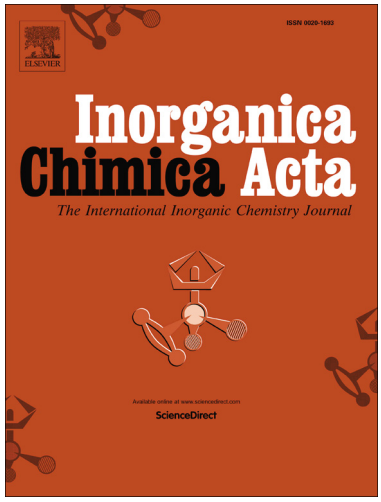

Research paper

DNA(CT), Protein(BSA) binding studies, anti-oxidant and cytotoxicity studies of new binuclear Ni(II) complexes containing 4(N)- substituted thiosemicarbazones

G. Kalaiarasi, C. Umadevi, A. Shanmugapriya, P. Kalaivani, F. Dallemer, R. Prabhakaran

PII: S0020-1693(16)30507-2
DOI: http://dx.doi.org/10.1016/j.ica.2016.09.006
Reference: ICA 17251

To appear in: *Inorganica Chimica Acta*

Received Date: 27 June 2016
Revised Date: 1 September 2016
Accepted Date: 5 September 2016

Please cite this article as: G. Kalaiarasi, C. Umadevi, A. Shanmugapriya, P. Kalaivani, F. Dallemer, R. Prabhakaran, DNA(CT), Protein(BSA) binding studies, anti-oxidant and cytotoxicity studies of new binuclear Ni(II) complexes containing 4(N)- substituted thiosemicarbazones, *Inorganica Chimica Acta* (2016), doi: http://dx.doi.org/10.1016/j.ica.2016.09.006

DNA(CT), Protein(BSA) binding studies, anti-oxidant and cytotoxicity studies of new binuclear Ni(II) complexes containing 4(N)- substituted thiosemicarbazones

G. Kalaiarasi,[a] C. Umadevi,[a] A. Shanmugapriya,[a] P. Kalaivani,[b] F. Dallemer [c] and R. Prabhakaran [a*]

[a] *Department of Chemistry, Bharathiar University, Coimbatore 641 046, India*
[b] *Department of Chemistry, Nirmala College for Women, Bharathiar University, Coimbatore 641018*
[c] *Laboratoire Chimie Provence-CNRS UMR7246, Université of Aix-Marseille I, II and III – CNRS, Campus Scientifique de Saint-Jérôme, Avenue Escadrille Normandie-Niemen, F-13397 Marseille Cedex 20, France*

Abstract

Four New Ni(II) complexes $[Ni_2(Msal\text{-}tsc)_2(\mu\text{-}dppm)]$ (**1**), $[Ni_2(Msal\text{-}mtsc)_2(\mu\text{-}dppm)]$ (**2**), $[Ni_2(Msal\text{-}etsc)_2(\mu\text{-}dppm)]$ (**3**) and $[Ni_2(Msal\text{-}ptsc)_2(\mu\text{-}dppm)]$ (**4**) containing 3-methoxy-salicylaldehyde-4(N)-substituted thiosemicarbazones having the general formula [H_2-MSal-tsc-R],(where R=H, Me, Et or Ph) and 1,1′-bis(diphenylphosphino)methane (dppm) were synthesized and characterized by various spectral, analytical techniques and X-ray crystallography. Crystallographic studies of the complexes **1** and **3** revealed the square planar geometry around the nickel ion. The binding ability of the complexes with CT-DNA was carried out by absorption / emission titration and which an intercalative mode of binding was observed. Further, their ability to interact with BSA protein has been explored. Investigations of antioxidation properties showed that all the compounds have strong radical scavenging properties. Further, anticancer activity of the compounds on the lung cancer cell line A549 has also been investigated. From the results it is observed that the complexes (**2** (IC_{50}=23 μM)**, 3** (IC_{50}=12 μM) & **4** (IC_{50}=20 μM)) exhibited a significant anticancer activity over complex **1**(IC_{50}=26 μM), ligands, $NiCl_2.6H_2O$ and the standard drug, Cisplatin(IC_{50}=25 μM).

Keywords: Nickel(II) thiosemicarbazones; Spectroscopy; X-ray crystallography; CT-DNA/BSA binding; Anti-Oxidant activity; Cytotoxicity;

Corresponding author. Tel.: +91-422-2428319; Fax: +91-422-2422387.

E-mail address: rpnchemist@gmail.com (R. Prabhakaran)

1. Introduction

Thiosemicarbazones are an important class of compounds due to their promising pharmacological properties, such as trypanocidal activity [1], antitubercular activity [2], and antitumor activities [3,4]. In recent years, a number of thiosemicarbazone derivatives have been synthesized and their antitumor activity against a broad spectrum of chemotherapeutic properties were also evaluated [5,6]. Moreover, the complexes consisted of transition metals and thiosemicarbazone ligands usually possess more potent pharmacological effects than the thiosemicarbazone ligands alone [7,8]. Some thiosemicarbazones have shown to increase their biological activity by their ability to form chelates with specific metal ions [9]. Among the transition metals, nickel, being a essential element because several hydrogenases and carbon monoxide dehydrogenases [10] contain such nickel ion as their active site. Nickel(II) thiosemicarbazone complexes has been more extensively studied and their anticancer, antifungal and antibacterial activities were reported [11-16]. Phosphines are one of the most important classes of ligands [17]. The design of polydentate phosphines to impose specific coordination geometries upon one or more metal centers has been an active area of research for the last three decades [18]. Though the synthesis of new chelating bis(phosphines) and the development of their metal complexes is an important area in the field of catalysis [19], however their biological properties were relatively unexplored. The development of multinuclear complexes as anticancer agents has recently generated tremendous interest [20]. The development of transition metal complexes with DNA binding ability has been an active area of research due to their potential use as drugs, regulators of gene expression and DNA structural probes [21-31]. Metal complexes show their anticancer effects through binding to DNA. Generally DNA is the primary intracellular target of anti-cancer drugs, so the interaction between small molecules and DNA can often cause DNA damage in cancer cells, blocking the division of cancer cells and resulting in cell death [32,33]. In addition to study the interaction of metal complexes with DNA, it is also equally important to study the binding behaviour of metal complexes with albumin proteins because of the fact that many drugs, including anticancer, anti-inflammatory, and general anesthetics, are transported in the blood by combining with serum albumin [34]. The studies on interaction of protein with metal complexes can provide information of the structural features that determine the therapeutic effectiveness of the complex and have become an interesting field in recent years [35]. Therefore, it is absolutely essential and interest to study the interaction behaviors of the metal complexes with DNA and protein (bovine serum albumin). It is also known that the

uncontrolled production of free radical reactive oxygen species such as superoxide anion can induce DNA damage in humans. Such a damage to DNA has been suggested to contribute to aging and various diseases including cardiovascular, cancer and chronic inflammation[36,37]. This has prompted us to test the synthesized complexes as free radical scavengers against DPPH radical, superoxide anion radical and Fe^{2+}ion. Further, the in vitro anticancer activities of the compounds were also determined using MTT (3-(4,5-dimethylthiazol-2-yl)-2,5-diphenyl-2H-tetrazolium bromide) assay against human lung cancer cell line (A549). In this line, analogues nickel complexes are found to be potent in various therapeutic applications [38-40]. With the above objectives in mind, herein we are reporting the synthesis, characterization, crystallography, DNA, protein binding, antioxidant and cytotoxicity studies of new binuclear nickel(II) complexes containing thiosemicarbazones and 1,1′ bis(diphenylphosphino)methane.

2. Results and discussion

2.1 Synthesis of new nickel(II) complexes

The reactions of two equivalents [$NiCl_2.6H_2O$] with two equivalents of 3-methoxy-4(N)-substituted thiosemicarbazones $(H_2L)^{1-4}$ and one equivalent 1,1′-bis(diphenylphosphino)methane [dppm] in 1:1 ethanol/dichloromethane resulted in the formation of new complexes **1-4** (Scheme 1), where the substituted thiosemicarbazones acted as a tridentate ONS donor ligand. The analytical data of which confirmed the stoichiometry of the complexes [Ni_2(Msal-tsc-R)$_2$(μ-dppm)] (where R= H, CH_3, C_2H_5 and C_6H_5). The structures of the complexes (**1** and **3**) were confirmed by the X-ray crystallography. The new complexes (**1–4**) are soluble in common organic solvents such as dichloromethane, chloroform, benzene, acetonitrile, ethanol, methanol, dimethylformamide and dimethylsulfoxide.

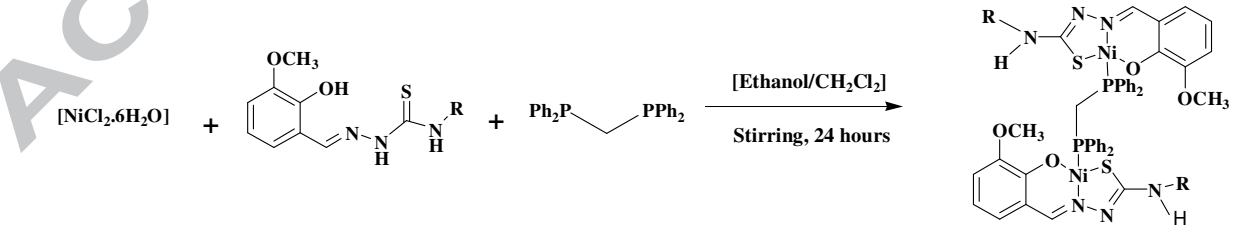

R = H **(1)**
R = CH_3 **(2)**
R = C_2H_5 **(3)**
R = C_6H_5 **(4)**

Scheme 1. Synthesis of new Ni(II) complexes

2.2 Spectroscopic Studies

The infrared spectra of the ligands $(H_2L)^{1–4}$ exhibited $\nu_{(OH)}$ vibration in the region 3310–3458 cm^{-1}, which disappeared completely upon complexation with nickel showing deprotonation prior to coordination through oxygen atom in all the four complexes (**1–4**). It is further confirmed with the upfield shift of 33-50 cm^{-1} for $\nu_{(C–O)}$ [41,42]. An azomethine nitrogen $\nu_{(C=N)}$ band appeared at the region 1536–1593 cm^{-1} in the ligands has been shifted to higher frequency in all the complexes (1592-1611 cm^{-1}) indicating the coordination of azomethine nitrogen atoms [41]. A sharp band appeared at 771-795 cm^{-1} corresponding to a $\nu_{C=S}$ vibration in the ligands disappeared completely in all the complexes and a new band appeared around 731–738 cm^{-1} corresponding to a possible $\nu_{C–S}$ vibration, indicating coordination of a thiolate sulphur atom after enolisation followed by deprotonation [41-43]. Moreover, the characteristic absorption bands corresponding to the presence of diphenylphosphinomethane were also present in the expected region [44,45]. The electronic spectra of nickel(II) complexes displayed two to four bands in the region around 263-418 nm (Fig. S1). The band appeared at 263-268 nm has been assigned to intra ligand transition and the bands at 313-371 nm to LMCT ($^3A_{2g} \rightarrow {}^3T_{2g}$) and the shoulder at 418-429 nm to forbidden ($^3A_{2g} \rightarrow {}^3T_{1g}$) transition [42,45]. The ^{1}H-NMR spectra of the ligands $(H_2L)^{1–4}$ and the corresponding complexes (**1-4**) recorded in DMSO and $CDCl_3$ at the field strength of 400 MHz showed all the expected signals (Fig. S2-S9). In the spectra of $(H_2L)^{1–4}$, a sharp singlet corresponding to the phenolic –OH group has appeared at δ 11.34-11.76 ppm. However, this singlet completely disappeared in all the complexes confirmed the involvement of phenolic oxygen in coordination [41,43,46]. The spectra of $(H_2L)^{1–4}$ showed a singlet at δ 9.13-10.0 ppm corresponding to (N(2)H-C=S) group [41,43], but in the complexes **1-4** there was no resonance attributable to N(2)H, indicating the coordination of thiolate sulphur atom of the ligand in the anionic form after deprotonation at N(2) [41,46]. In the spectra of $H_2L^{1–4}$ and the complexes, a complex multiplet appeared at δ 6.3–7.98 ppm was assigned to aromatic protons of the ligands and diphenylphosphinomethane [41,43] and a singlet corresponding to the $–OCH_3$ group occurred at δ 3.59–3.81 ppm range [41,43]. Two singlets observed at δ 8.37–8.50 ppm and δ 8.37–9.20 ppm have been assigned to azomethine and terminal -NH protons of the ligands $(H_2L)^{2–4}$ [41,43]. Two broad singlets appeared at δ 7.8 and δ 8.0 ppm corresponding to NH_2 protons of H_2L^1 [41]. Whereas, in the complexes a singlet at δ 4.45 - 5.29 ppm was assigned to the terminal NH protons of the ligands. Though the spectra of **1** and **4** showed a doublet at δ 7.835- 7.857 & δ 8.122–8.144 ppm corresponding to the

azomethine proton [41], the same has been mixed in the aromatic region for **2** and **3**. In the spectra of H_2L^2 and the complex **2**, a doublet was observed around δ 2.91–2.99 ppm due to the methyl group of protons. A triplet observed around δ 1.13–1.14 ppm in the spectra of H_2L^3 and the complex **3**, was assigned to the presence of methyl group of protons [41]. Further, a multiplet at δ 3.25 –3.58 ppm was also observed corresponding to the methylene protons of H_2L^3 and complex **3** [41]. In addition, a triplet was observed in the spectra of all the complexes at δ 4.0-4.16 ppm due to the presence of methelene protons of the 1,1′-bis(diphenylphosphino)methane ligand [44].

2.3 X-ray crystallography

In order to confirm the exact structure of the complexes, X-ray crystallographic analyses has been done for the new complexes (**1** and **3**). Complex **1** and **3** crystallized in the monoclinic space group P_{21}. The crystallographic data, selected bond distances and angles are listed in Tables 1 and 2. In the dimeric complexes **1** and **3**, each nickel atom is coordinated by a tridentate binegative ligand through phenolic oxygen, N1 hydrazinic nitrogen and thiolate sulphur atom by forming a six member and another five member ring with Ni–S bond distances of 2.1370(7) Å and 2.139(1) Å, respectively, Ni–O bond distances of 1.838(2) Å and 1.852(2) Å, respectively and Ni–N bond distances of 1.884(2) Å and 1.885(3) Å, respectively [42,43]. The remaining binding site is occupied by the phosphorous atom of 1,1′-bis(diphenylphosphino)methane unit with (Ni(1)–P(1)) bond distances of 2.1974(5) Å and 2.2075(8) Å, respectively) [45] with the bite angle [S(1)–Ni(1)–N(1)] of 87.68(5)° for **1** and 86.88(9) ° for **3**. The [S(1)–Ni(1)–O(1)] bond angles found are 174.66(5) ° for **1** and 174.48(8) ° for **3** [42,43] and [P(1)–Ni(1)–N(1)] bond angles found are 174.99(5) ° for **1** and 176.95(9) ° for **3** [45] which deviate considerably from the ideal angle of 180 ° causing significant distortion in the square planar geometry of the complexes. Two of these symmetrical units are bridged through dppm ligand in the complexes **1** and **3**.

In complex **1,** an intermolecular hydrogen bonding was found between the imine nitrogen and the oxygen atom [N(2)...O(5) (2.863 A˚)] of the water which came through the solvent of crystallization (Fig. S10). The presence of four intermolecular hydrogen bondings in complex **3** creates a 2D network (Table S1). First two hydrogen bonding comes through interaction N(2) and N(5) nitrogen atoms of the coordinated thiosemicarbazone moieties and with the hydrogen atoms of water molecule which is coming through solvent of crystallisation (Fig. S11). The third intermolecular hydrogen bonding is between hydrogen

atom of N(3) terminal nitrogen atom and oxygen atom of methanol which is used as solvent for crystallisation and the fourth hydrogen bonding is between water and methanol moieties of crystallisation solvents. All the above four intermolecular hydrogen bonding led give 2D layer structure to the complex **3**.

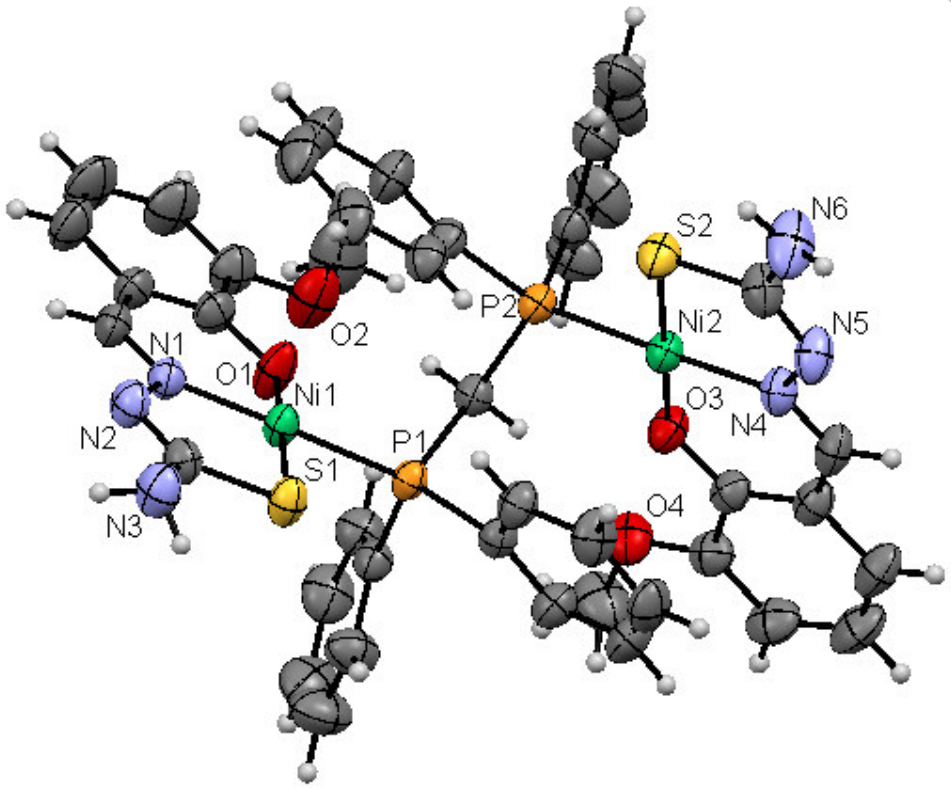

Fig. 1. ORTEP diagram of $[Ni_2(Msal\text{-}tsc)_2(\mu\text{-}dppm)]$ (**1**)

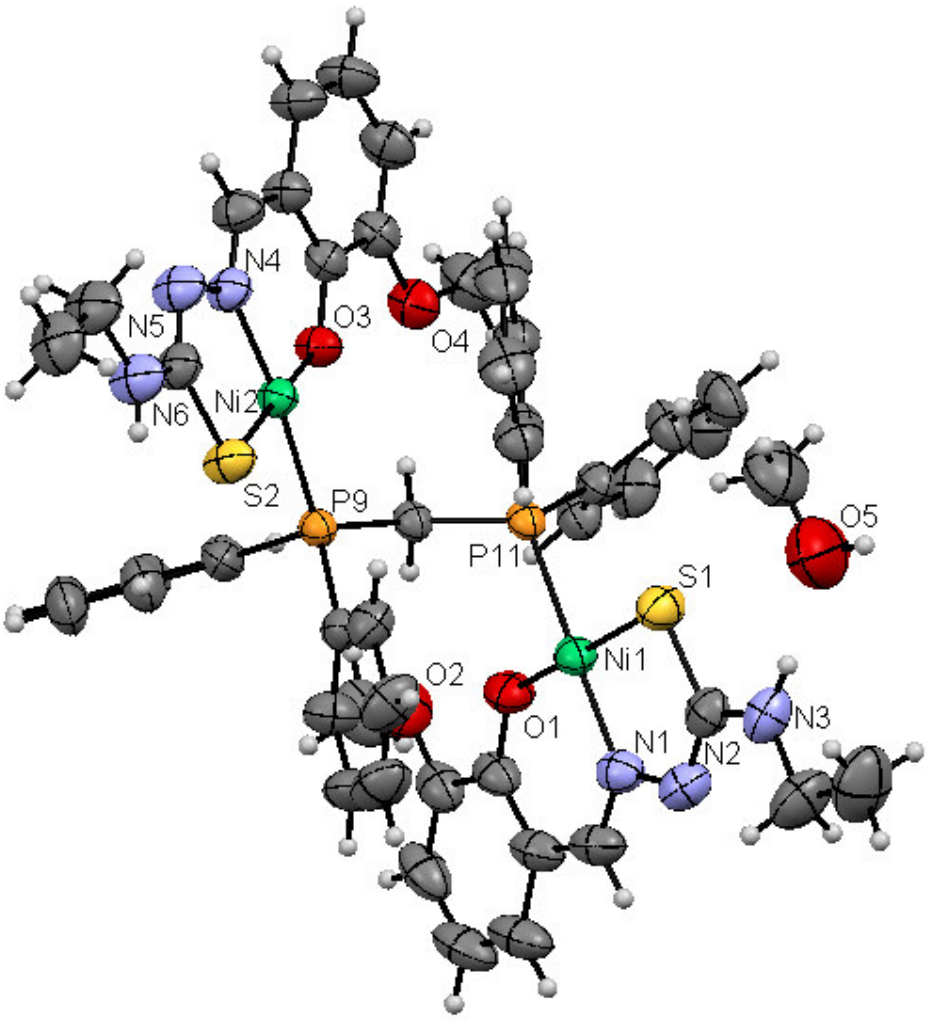

Fig. 2. ORTEP diagram of [Ni_2(Msal-etsc)$_2$(μ-dppm)] (**3**)

Table 1. Crystallographic data of complexes **1** and **3**

Identification code	$[Ni_2(Msal\text{-}tsc)_2(\mu\text{-}dppm)]$(**1**)	$[Ni_2(Msal\text{-}etsc)_2(\mu\text{-}dppm)]$(**3**)
Empirical formula	$C_{43}H_{40}N_6Ni_2O_4P_2S_2$	$C_{47}H_{48}N_6Ni_2O_4P_2S_2$
Formula weight	984.32	1072.46
Temperature	293(2) K	293(2) K
Wavelength	1.54184 Å	1.54184 Å
Crystal system	Monoclinic	Monoclinic
Space group	$P2_1/C$	$P2_1/C$
Unit cell dimensions		
a	11.3353(9) Å	10.55971(13) Å
B	14.0555(10) Å	15.68622(13) Å
C	28.3292(2) Å	31.4025(3) Å
α	90°	90°
β	94.3615(7)°	94.1646(9)°
γ	90°	90°
Volume	4500.44 $Å^3$	5187.84$Å^3$
Z	4	4
Density	1.453 Mg/m^3	1.373 Mg/m^3
Absorption coefficient,	3.020 mm^{-1}	2.678 mm^{-1}
F(000)	2040	2240
Crystal size	0.16 × 0.16 × 0.07 mm	0.16 × 0.16 × 0.12 mm
Crystal shape	Block	Block
θ range for data collection	4.421 to 73.635°	4.182 to 73.606°
Limiting indices	$-13 \le h \le 13$, $-16 \le k \le 17$, $-34 \le l \le -35$	$-12 \le h \le 12$, $-19 \le k \le 19$, $-39 \le l \le 38$
Reflections collected	20206	23092
Independent reflections	8894 (*R*(int) = 0.0339)	10291(*R*(int) = 0.0270)
Completeness to θ	66.97° 99.62 %	66.97° 99.89 %
Absorption correction	multi-scan	multi-scan
Refinement method	Full-matrix least-squares on F^2	Full-matrix least-squares on F^2
Data / restraints / parameters	8894 / 0 / 567	10291/ 0/631
Goodness-of-fit on F^2	1.024	1.138
Final *R* indices [$I>2\sigma(I)$]	R1 = 0.0331, wR2= 0.0875	R1 = 0.0508, wR2 = 0.1383
R indices (all data)	R1 = 0.0366, wR2 = 0.0910	R1 = 0.0542, wR2 = 0.1410

Table 2: Selected bond lengths(Å) and bond angles(°) of the complexes **(1)** and **(3)**

BOND LENGTHS	**1**	**3**
Ni(1)-S(1)	2.1370(7)	2.139(1)
Ni(1)-P(1)	2.1974(5)	2.2075(8)
Ni(1)-O(1)	1.838(2)	1.852(2)
Ni(1)-N(1)	1.884(2)	1.885(3)
Ni(2)-S(2)	2.1410(6)	2.1254(9)
Ni(2)-P(2)	2.1968(6)	2.1254(9)
Ni(2)-O(3)	1.850(1)	1.862(2)
Ni(2)-N(4)	1.885(2)	1.881(3)
BOND ANGLES		
S(1)-Ni(1)-P(1)	96.27(2)	94.58(4)
S(1)-Ni(1)-O(1)	174.66(5)	174.48(8)
S(1)-Ni(1)-N(1)	87.68(5)	86.88(9)
P(1)-Ni(1)-O(1)	81.01(5)	83.42(7)
P(1)-Ni(1)-N(1)	174.99(5)	176.95(9)
O(1)-Ni(1)-N(1)	94.79(7)	94.9(1)
S(2)-Ni(2)-P(2)	94.99(2)	91.58(3)
S(2)-Ni(2)-O(3)	176.54(5)	177.52(7)
S(2)-Ni(2)-N(4)	87.32(5)	87.01(8)
P(2)-Ni(2)-O(3)	82.59(5)	86.21(7)
P(2)-Ni(2)-N(4)	175.61(6)	173.32(8)
O(3)-Ni(2)-N(4)	94.94(7)	95.1(1)

2.4 DNA binding studies

The interaction between DNA and metal complexes is of paramount importance in understanding the mechanism of any drug action. Thus, the mode and propensity for binding of the new nickel(II) complexes **1-4** to CT DNA were studied with the help of electronic absorption and fluorescence quenching techniques. The stability of the complexes in DMSO, 1% aqueous DMSO and tris-HCl buffer have been carried out by using UV-Vis spectrophotometer. The results showed that all the complexes are stable in these solutions allowing us to proceed further for DNA binding studies. The absorption spectra of the complexes (**1–4**) at constant concentration (10 μM) in the presence of different concentrations of CT-DNA (5–50 μM) are given in Fig. 3.

The absorption spectra of complex **1** consist of three resolved bands centered at 284 nm (intraligand transition), 373 and 425 nm (charge transfer). As the DNA concentration is increased, hypochromism (A=0.3099–0.1563) with a red shift of 2 nm (up to 286 nm) was observed in the intraligand band. The CT band at 373 and 425 nm showed modest hypochromism (A=0.1685–0.0912 and A=0.0990-0.0550 respectively) with negligible shifts

in the wavelength. The binding behavior of complexes **2, 3** and **4** is also quite similar. Complex **2** exhibited hypochromism in the intraligand band at 265 nm (A=0.7609–0.2771) with 1 nm red shift and hypochromism at 367 nm with 1 nm red shift (LMCT) (A=0.4323–0.1371). Complex **3** exhibited hypochromism in the intraligand band at 304 nm (A=0.6458–0.3818) with 1 nm red shift and hypochromism at 369 nm (LMCT) (A=0.2842–0.1433). The spectra of complex **4** consist of two resolved bands centered at 262 nm and 308 nm (intraligand transition). As the DNA concentration is increased, hypochromism (A=0.2876–0.1748) with a red shift of 1 nm was observed in the intraligand band. The another IL band at 308 nm (A=0.3250–0.2016) showed hypochromism with negligible shifts in the wavelength. The observed hypochromic effect with a red shift suggested that the new complexes may bind to CT-DNA by intercalation. Further, the binding mode has been evidented through competitive binding studies using Ethidium Bromide (EB)

The intrinsic binding constant K_b is a useful tool to monitor the magnitude of the strength with the compounds which bind to CT-DNA (Table 3). It can be determined by monitoring the changes in the absorbance in the intraligand band at the corresponding λ_{max} with increasing concentration of DNA and is given by the ratio of slope to the 'y' intercept in plots of [DNA]/(ε_a-ε_f) versus [DNA] (Fig. 4) [43].

To further confirm the interaction between complexes **1–4** and CT-DNA, competitive binding studies using Ethidium Bromide (EB) were conducted. The emission intensity of EB is used as a structural probe as EB shows reduced emission intensity in buffer solution due to either solvent quenching or photoelectron transfer mechanism[47] and enhancement in the emission intensity when it bound intercalatively to DNA. While adding the complexes **1–4** to DNA pretreated with EB, the DNA-induced emission intensity at 604 nm was decreased (Fig. S12). This indicates the replacement of EB by complexes from the EB–DNA system. Such a characteristic change is often observed in intercalative DNA interactions. The quenching extents of complexes **1-4** were evaluated qualitatively by employing Stern–Volmer equation (1).

$$I_o/I = K_{sv}[Q] + 1 \qquad (1)$$

Where I_o is the emission intensity in the absence of compound, I is the emission intensity in the presence of compound, K_{sv} is the quenching constant, and [Q] is the concentration of the compound. The Stern–Volmer quenching constant K_{SV}, obtained as the slope of I_o/I versus the concentration of the quencher (Table 3) (Fig.S13). A decrease in the

emission intensity suggests stronger binding affinity of the complexes to CT-DNA [43,48]. Furthermore, the observed quenching constants and binding constants of the new complexes suggested an intercalative binding mode the complexes to DNA.

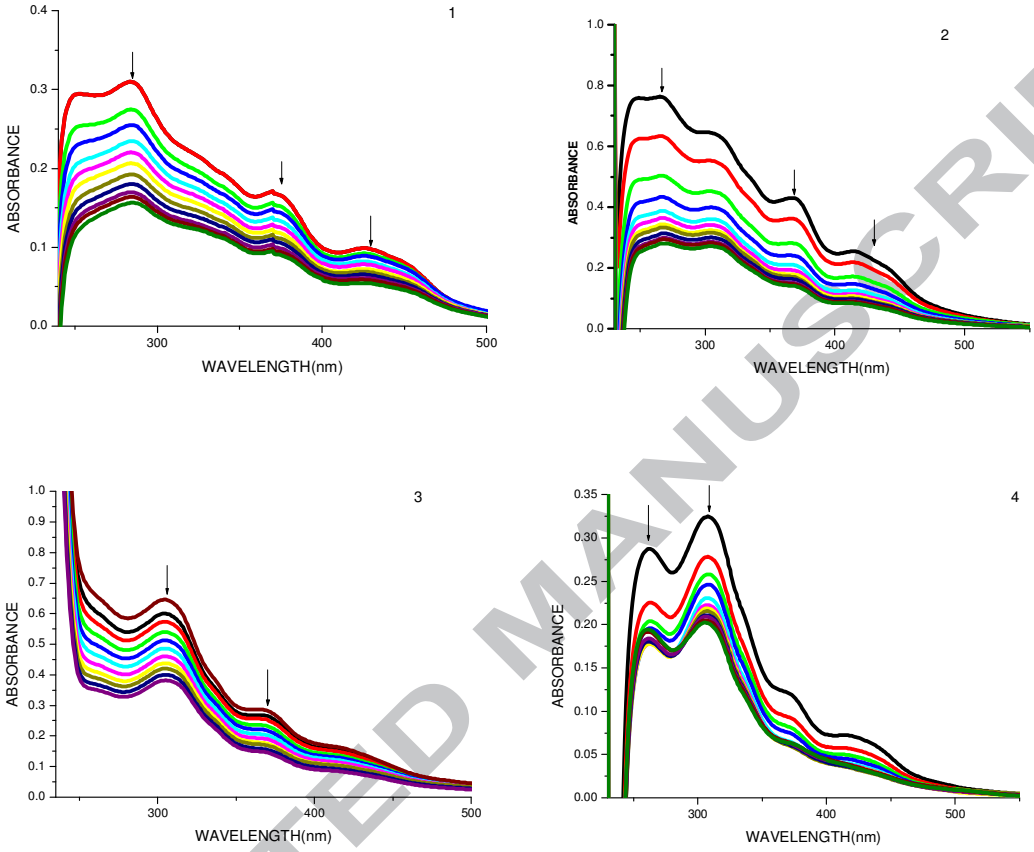

Fig. 3. Changes in the electronic absorption spectra of complexes **1-4** (10 μM) with increasing concentrations (5-50 μM) of CT-DNA (tris HCl buffer, pH 7.2).

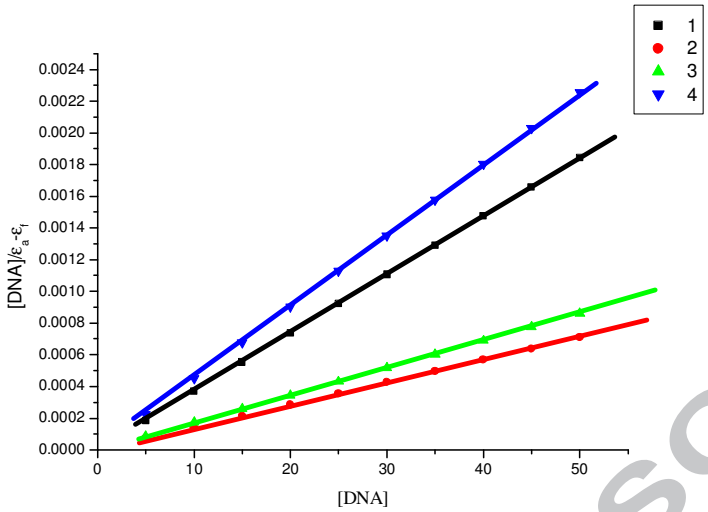

Fig. 4. plot of [DNA]/(ε_a-ε_f) versus [DNA]

Table 3 :The K_b and K_{sv} values for the interactions of complexes (**1–4**) with CT-DNA

Complex	K_b/M^{-1}	K_{SV}/M^{-1}
1	$2.765\pm0.120\times10^5$	$5.99\pm0.029\times10^3$
2	$1.079\pm0.050\times10^5$	$6.79\pm0.021\times10^3$
3	$4.311\pm0.056\times10^5$	$8.67\pm0.034\times10^3$
4	$3.384\pm0.140\times10^5$	$6.85\pm0.026\times10^3$

2.5 Protein binding studies

2.5.1 Quenching mechanism of BSA by complexes

Binding of Schiff base metal complexes with the most abundant carrier proteins (serum albumins) have also been an area of interest as such drug–protein binding greatly influences absorption, drug transport, storage, metabolism and excretion properties of typical drugs in vertebrates [49]. Since serum albumins are well known to bind with small aromatics, the possible binding interactions of the nickel(II) thiosemicarbzone complexes (**1-4**) with BSA have been investigated by absorption/emission-titration experiments at room temperature. Prior to the interaction fluorescence studies, the stability of complexes (**1-4**) was studied in DMSO, 1% aqueous DMSO and in phosphate buffer using UV-Vis spectrophotometer. All the complexes were found to be stable in these solutions for, at least, 24 h, allowing us to carry on with the studies with albumin. In the absorption spectra of BSA,

the addition of 10 μM concentrations of the four complexes (**1-4**) (Fig. S14) showed enhanced absorption intensity of BSA with a blue shift of complex–BSA spectrum (from 265 to 261 nm). The formation of non-fluorescence ground-state complex induced the change in absorption spectrum of fluorophore and possible quenching mechanism of BSA by complexes (**1-4**) was found as static quenching [50].

2.5.2. Fluorescence quenching studies of BSA

A solution of BSA (10 μM) was titrated with various concentrations of the complexes (0–100 μM). Fluorescence spectra were recorded in the range of 290–500 nm upon excitation at 280 nm. The changes observed on the emission spectra of BSA by the addition of increasing amounts of the complexes (**1-4**) which are shown in Fig. 5.

Upon the addition of complexes **1–4** to BSA, a significant decrease in the fluorescence intensity was observed at 346 nm with hypochromism of 8.98 %, 10.33 %, 13.95 % and 3.04 % respectively accompanied by 1-4 nm blue shifts. The observed quenching may be attributed to the possible changes in secondary structure of protein and this indicating the binding of complex to BSA [22]. According to Stern–Volmer quenching equation, eq 1. The K_{SV} value was found to be 8.75±0.021 x 10^3 M^{-1}, 9.23±0.016 x 10^3 M^{-1},1.367±0.036 x 10^4 M^{-1} and 4.09±0.009 x 10^3 M^{-1} corresponding to complexes **1**, **2**, **3** and **4** respectively. The observed linearity in the plots (Fig. 6; Table 4) indicates the ability of the complexes to quench the emission intensity of BSA. From K_{SV} values, the complex **3** exhibited better protein-binding. For the static quenching interaction, if it is assumed that there are similar and independent binding sites in the biomolecule, the binding constant (K_b) and the number of binding sites (n) can be determined according to the method [51] using the Scatchard equation (2).

$$\log [(F_o - F)/F] = \log K_b + n \log [Q] \qquad (2)$$

where, in the present case, K_b is the binding constant for the complex–protein interaction and 'n' is the number of binding sites per albumin molecule, which can be determined by the slope and the intercept of the double logarithm regression curve of log $[(F_o - F)/F]$ versus log[Q] (Fig. 7; Table 4).

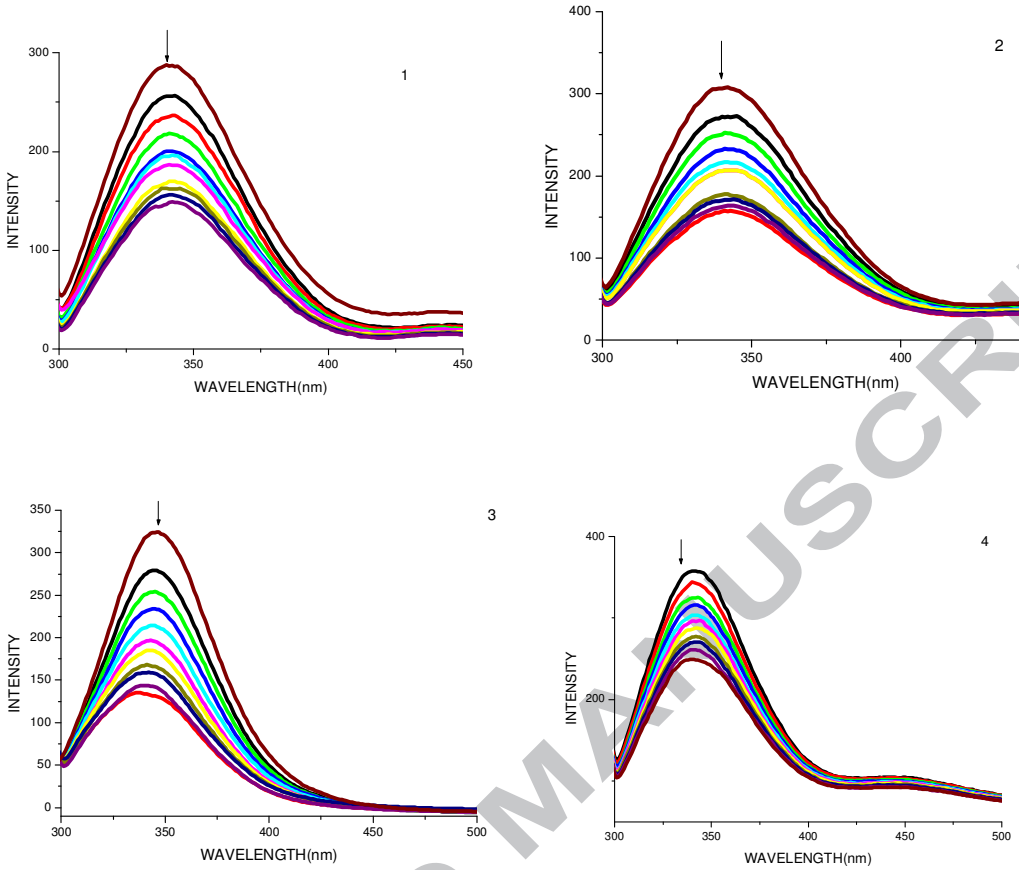

Fig. 5. The emission spectra of BSA (10 μM; λ_{exc}= 280 nm; λ_{emi}= 346 nm) in the presence of increasing amounts of complexes **1-4** (0–100 μM). The arrow shows the emission intensity changes upon increasing complex concentration.

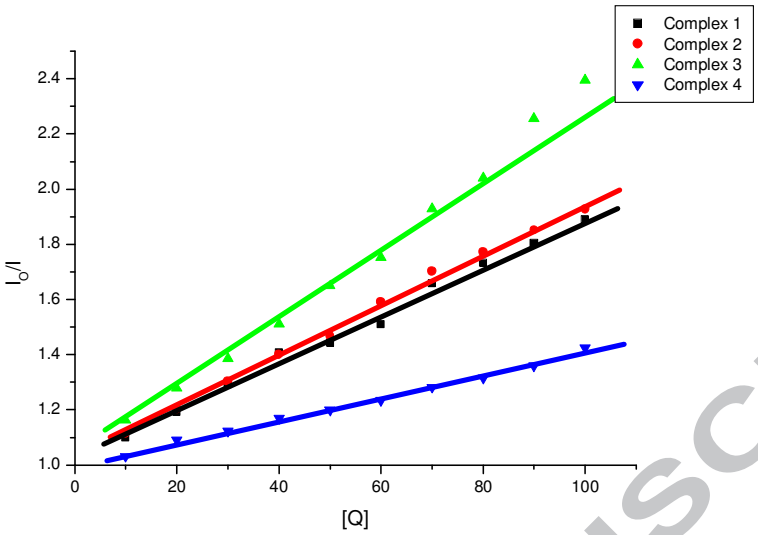

Fig. 6. Stern–Volmer plot of the fluorescence titration of the complexes (**1-4**) (10-100 µM) with BSA (10 µM).

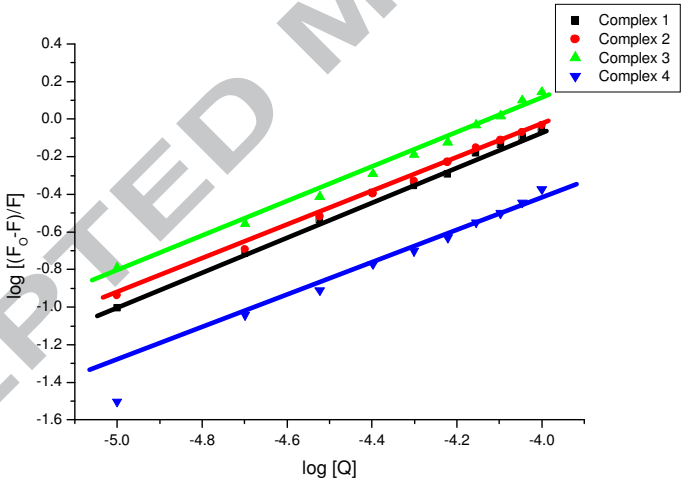

Fig. 7. Scatchard plot of the fluorescence titration of the complexes (**1-4**) (10-100 µM) with BSA(10 µM).

Table 4: Quenching constant (K_{sv}), binding constant (K_{bin}) and number of binding sites (n) for the interactions of complexes (**1–4**) with BSA

Complex	K_{SV}/M^{-1}	K_{bin}/M^{-1}	'n'
1	$8.75\pm0.021\times10^3$	$5.637\pm0.020\times10^3$	0.9499
2	$9.23\pm0.016\times10^3$	$4.747\pm0.011\times10^3$	0.9262
3	$13.67\pm0.036\times10^3$	$7.584\pm0.017\times10^3$	0.9422
4	$4.09\pm0.009\times10^3$	$7.097\pm0.018\times10^3$	1.0574

2.5.3. Synchronous fluorescence spectroscopic studies of BSA:

Synchronous fluorescence spectral study involves simultaneous scanning of the excitation and emission monochromators while maintaining a constant wavelength interval between them. It was used to obtain information about the molecular environment in the vicinity of the fluorophore moieties of BSA [52]. Synchronous fluorescence spectra show tyrosine residues of BSA only at the wavelength interval $\Delta\lambda$ of 15 nm whereas tryptophan residues of BSA at $\Delta\lambda$ of 60 nm. While the amount of complexes (**1-4**) added to BSA (10 μM) is increased, there is a decrease in the fluorescence intensity of the complexes **1** and **4** and increase in the fluorescence intensity of the complexes **2** and **3** corresponding to tyrosine residue with a red shift (1-3 nm) (Fig. S15) was noted. In addition, significant decrease in fluorescence intensity of tryptophan residues together with a small blue shift (1 nm) in the emission wavelength was also observed for the complexes (Fig. S16). These experimental results indicate that the metal complexes affect the microenvironment of both tyrosine and tryptophan residues during the binding process and synchronous measurements confirmed the effective binding of all the complexes with BSA.

2.6 Antioxidant capacity

Since the experiments conducted so far revealed that the complexes exhibit significant DNA and protein binding affinity, it is considered worthwhile to study the antioxidant activity of these compounds. Free radicals play an important role in the inflammatory process. Thus, compounds with possible antioxidant properties could play a crucial role against inflammation and lead to potentially effective drugs. Antioxidants that exhibit radical scavenging activity are receiving increased attention since they present interesting anticancer, anti-ageing and anti-inflammatory activities. Therefore, compounds with antioxidant properties may offer protection against rheumatoid arthritis and inflammation.[45] The radical scavenging activities of our compounds along with standards, such as ascorbic acid and

butylated hydroxytoluene (BHT) in a cell free system, have been examined with reference to DPPH radicals (DPPH˙) and superoxide anion radicals ($O_2^{-\cdot}$) and their reducing power and total antioxidant activity were examined.The power of the compounds ability to scavenge various radicals was found to be slightly higher than that of the standard antioxidants (Ascorbic acid and BHT).

The free radical scavenging activity of $NiCl_2.6H_2O$, ligands, 1,1′-bis(diphenylphosphino)methane and new Ni(II) complexes were tested by its ability to bleach the stable radical DPPH. This assay provided information on the reactivity of the compound with a stable free radical. Because of the odd electron, DPPH shows a strong absorption band at 517 nm in the visible spectrum [53]. As this electron becomes paired off in the presence of a free radical scavenger, the absorption vanishes, and the resulting decolonization is stoichiometric with respect to the number of electrons taken up. The compounds represent moderate to significant reducing ability of DPPH radical when compared to the reference compound ascorbic acid. The new complexes exhibited a significant DPPH radical scavenging effect greater than that of well established vitamin C, a reference drug established elsewhere [45,54]. The free radical scavenging activity of the compounds increased with an increase in the concentration of the compounds and it is measured interms of IC_{50}values (Fig. 8 and 10; Table S2). Our results were compared with the literature data, the new binuclear Ni(II) complexes showed moderate scavenging activity.[45,55,56]

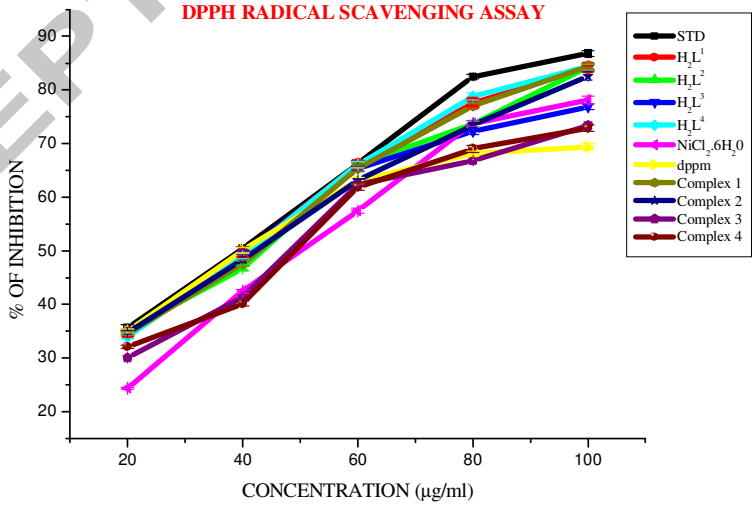

Fig. 8. DPPH scavenging activity of ligands, 1,1′-bis(diphenylphosphino)methane (dppm), $NiCl_2.6H_2O$ and new Ni(II) complexes. Error bars represent the standard deviation of the mean (n=3).

Superoxide ($O_2^{\cdot-}$) is highly reactive compound among the reactive oxygen species (ROS). These species can disintegrate cell membranes and damage protein and DNA structures and are largely responsible for many diseases, such as cancer, liver injury and cardiovascular complications[36]. The ability of Nickel chloride, ligands, 1,1′-bis(diphenylphosphino)methane and new Ni(II) complexes were appreciable for the superoxide radicals when compared to the standards (Table S2; Fig 9-10). It can be seen that the inhibitory effects of the tested compounds on $O_2^{\cdot-}$ is concentration related and the suppression ratio increases with the increasing sample concentration in the range of the tested concentration. As seen from the results, the compounds exhibited significant activity[57].

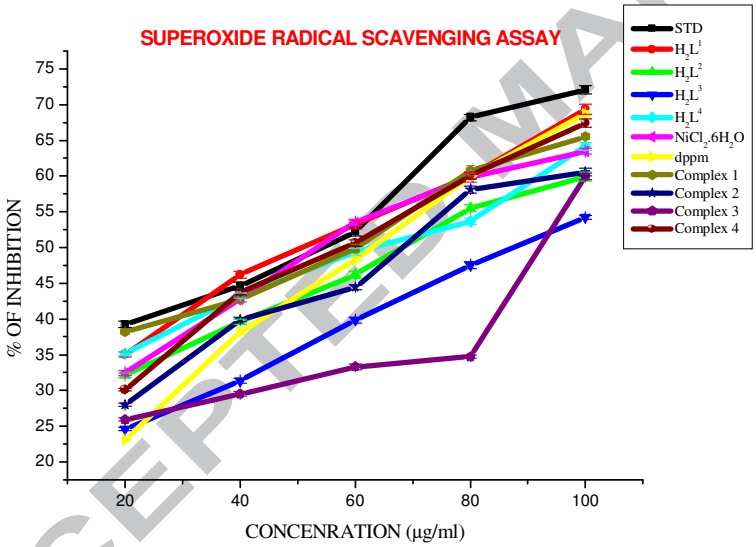

Fig. 9. Superoxide scavenging activity of ligands, bis(diphenylphosphino)methane (dppm), $NiCl_2.6H_2O$ and new Ni(II) complexes. Error bars represent the standard deviation of the mean (n=3).

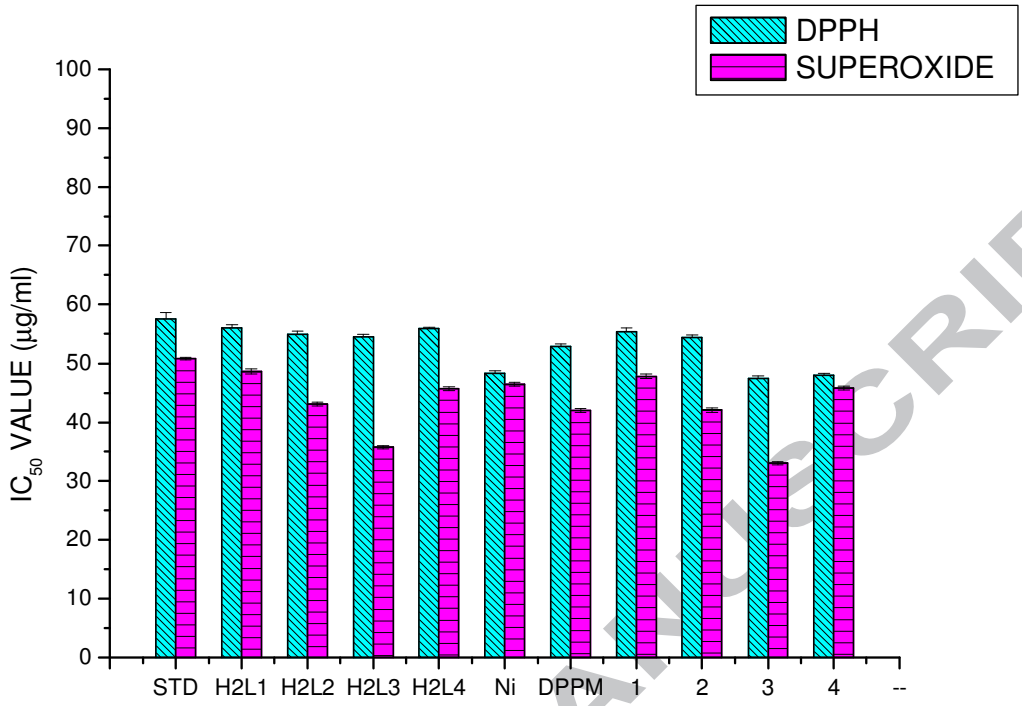

Fig. 10. Antioxidant activity (IC_{50} values) of ligands, bis(diphenylphosphino)methane (DPPM), $NiCl_2.6H_2O$ and new Ni(II) complexes . Error bars represent the standard deviation of the mean (n=3).

Fig. 11 shows the reducing power of $NiCl_2.6H_2O$, ligands, bis(diphenylphosphino)methane and new Ni(II) complexes as a function of their concentration. In this assay, the yellow color of the test solution changed to various shades of green and blue depending upon the reducing power of each compound. The presence of reducers (i.e., antioxidants) causes the reaction of the Fe^{3+}/ferricyanide complex to the ferrous form the Perl's Prussion blue after the addition of trichloroacetic acid and ferric chloride, that can be monitored at 700 nm. The reducing power of the standard BHT at various concentrations was higher than that of test compounds. The reducing power of test compounds solutions in DMSO increased with increase in concentration and showed absorbances nearer to those of the standard. All the metal complexes showed much better activity than the ligands, bis(diphenylphosphino)methane and Ni salt (Fig.11). Thus the coupling of metal ions with the ligands is the important features for increased reducing power

of these compounds[58]. The complex **3** has the highest antioxidant activity when compared to the other complexes as it showed the reducing power of 0.71±0.003/ 100µg ml^{-1} .

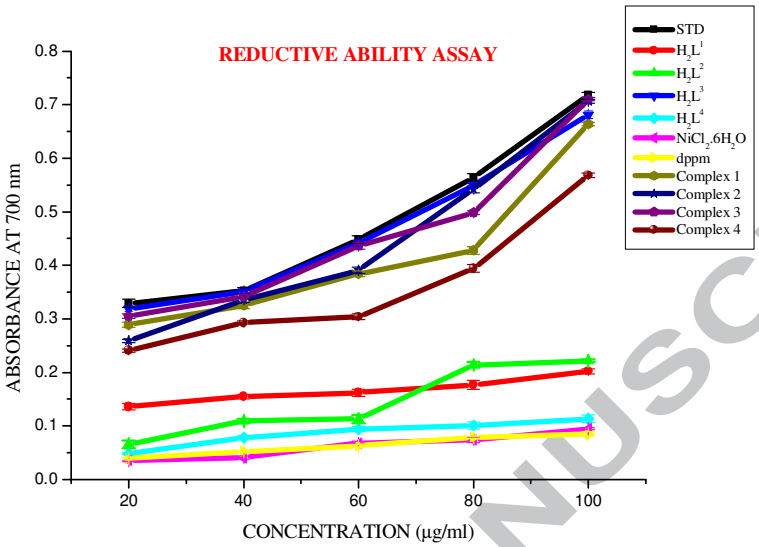

Fig. 11. Reductive ability of ligands, bis(diphenylphosphino)methane (dppm), $NiCl_2.6H_2O$ and new Ni(II) complexes. Error bars represent the standard deviation of the mean (n=3).

Among the complexes, total antioxidant capacity was found to be high in complex **3** and low in bis(diphenylphosphino)methane**.** (Table 5) Moreover, from the results obtained for the four Ni(II) complexes, complex **3** showed the better activity may be due to the ethyl substitution in the terminal nitrogen of the ligand. From the above results, it can be concluded that the scavenging effects of the nickel salt, bis(diphenylphosphino)methane and free ligands is significantly less when compared to their corresponding Ni(II) complexes, which is mainly due to the chelation of the organic ligand with the Ni(II) ion[55,56].

Table 5: Estimation of Total antioxidant capacity of ligands, bis(diphenylphosphino)methane (dppm), $NiCl_2.6H_2O$ and new Ni(II) complexes

Compounds	µg Ascorbic acid equivalents/ml
H_2L^1	9.84±0.04
H_2L^2	10.95±0.06
H_2L^3	9.52±0.05
H_2L^4	12.27±0.07
$NiCl_2.6H_2O$	13.66±0.11
dppm	7.87±0.04
Complex 1	10.57±0.04
Complex 2	25.33±0.05
Complex 3	35.08±0.03
Complex 4	16.14±0.06

2.7 Cytotoxic studies

MTT (3-(4,5-dimethylthiazol-2-yl)-2,5-diphenyltetrazolium bromide) assay

The positive results obtained from the previous biological studies namely, DNA binding, BSA binding and antioxidative studies of compounds encouraged us to test their cytotoxicity against human lung cancer cell line (A549). The tumour inhibiting capacity of the compounds against A549 cells (a model cell line for lung cancer) by the MTT assay, that is based on the mitochondrial reduction of the tetrazolium salt by actively growing cells to produce blue insoluble formazan crystals, was undertaken. Compounds were dissolved in DMSO and blank samples containing same volume of DMSO are taken as controls to identify the activity of solvent in this cytotoxicity experiment. Cisplatin was used as a positive control to assess the cytotoxicity of the test compounds. The results were analyzed by means of cell viability expressed as IC_{50} values are shown in Table 6. Appropriate Ligands, 1,1′-bis(diphenylphosphino)methane and $NiCl_2.6H_2O$ used in the synthesis of the complexes were also tested for cytotoxicity. Though the ligands and metal precursor showed moderate inhibiting activity against lung cancer cell line (A549), the new complexes exhibited significant activity against A549. The complexes exhibited good cytotoxic effects on lung cancer cells with lower IC_{50} values indicating their efficiency in killing the cancer cells even at low concentrations which confirmed that the chelation of the ligand with the Ni(II) ion is the only responsible factor for the observed cytotoxic properties of the new complexes. The Ni(II) complexes which possess better cytotoxic activities than ligand may be attributed to the extended planar structure induced by the π/π^* conjugation resulting from the chelating of the metal ion with ligand.Some promising cytotoxic effects were observed for new binuclear

Ni(II) complexes toward the A549 cell line as reported in Table 6 (Fig.S17). These results are much better than those previously reported for other mononuclear Ni(II) complexes [43]. The complex **3** showed higher cytotoxic effect followed by the complexes **4** and **2**. It is interesting to note that the complexes **2**, **3** and **4** exhibited significant activity than cisplatin. The highest activity was noted for the complex **3** and the least activity was observed with the complex **1**. In addition, though the ligand coordinated as bibasic tridentate to Ni(II) in all the complexes, the inhibitory activity of **3** against cancer cell is higher, which may be due to the electron donating ethyl substitution in the terminal nitrogen of the ligand.

Table 6: The IC_{50} values for the human lung cancer cell line A549 after an incubation period of 48 hours with the ligands, bis(diphenylphosphino)methane (dppm), $NiCl_2.6H_2O$ and new Ni(II) complexes

Complexes	IC_{50}value(μM)
	A549
H_2L^1	34±0.32
H_2L^2	29±0.26
H_2L^3	27±0.23
H_2L^4	30±0.28
$NiCl_2.6H_2O$	31±0.35
dppm	43±0.52
Complex 1	26±0.28
Complex 2	23±0.20
Complex 3	12±0.14
Complex 4	20±0.19
Cisplatin	25±0.23

3. Conclusion

New binuclear nickel(II) thiosemicarbazone complexes have been synthesized and characterized by various spectro and analytical techniques. The true nature of coordinating ligand with the central metal atom was established by X-ray crystallographic studies. From the study, it is inferred that in complexes **1** and **3** the ligands coordinated as tridentate bibasic nature. In order to study the potential binding ability of the new complexes, CT-DNA and BSA protein were taken as models. The complexes bind to CT-DNA through intercalation mode and with BSA, the quenching was found as static. Among the four complexes, complex **3** exhibited better binding affinity with BSA. All the complexes exhibited

significant antioxidant activity. The cytotoxic studies showed that the complexes **2, 3** and **4** exhibited good cytotoxic activity against A549 cell line and complex **1** showed IC_{50} cytotoxicity coefficients similar to those of cisplatin. The IC_{50} value of the complexes in A549 cell line was relatively low as compared with the standard *cisplatin* , ligands, 1,1′-bis(diphenylphosphino)methane, $NiCl_2.6H_2O$. Complex **3** exhibited relatively high cytotoxic activity against lung cancer A549 cells with low IC_{50} value(IC_{50} =12 μM) than the standard *cisplatin*. In general, complex **3** showed bettter biological activity in all the experiments. The substitution of an ethyl group at terminal nitrogen of the coordinated ligand of complex **3** may be responsible for its observed good biological activity over the other three complexes.

4. Experimental

4.1. Complex synthesis and characterization

1,1′ bis(diphenylphosphino)methane and $NiCl_2.6H_2O$ were purchased from Sigma Aldrich Ltd. The ligands $[H_2L]$[1-4] were synthesized according to the standard literature procedure [41]. All the reagents used were Analar grade, were purified and dried according to the standard procedure [59]. CT-DNA, EB and BSA were obtained from Himedia. Infrared spectra were measured as KBr pellets on a JASCO FT-IR 4100 instrument between 400–4000 cm^{-1}. Elemental analyses of carbon, hydrogen, nitrogen, and sulfur were determined by using Vario EL III CHNS at the Department of Chemistry, Bharathiar University, Coimbatore, India. Melting points were measured in a Lab India apparatus. The electronic spectra of the complexes have been recorded in DMSO using a JASCO V-630 Spectrophotometer in the 800–200 nm range. Emission spectra were recorded by using JASCO FP 6600 Spectrofluorometer. ^1H NMR spectra were recorded in DMSO and $CDCl_3$ at room temperature with a Bruker 400 MHz instrument, chemical shift relative to tetramethylsilane. Single crystal data collections and corrections for the new Ni(II) complexes (**1** and **3**) were done at 293 K with a CCD kappa Diffractometer using graphite monochromated MoKα (l = 1.54184 A˚) radiation [60]. The structural solutions were done by using SHELXS-97 [61] and refined by full matrix least square on F^2 using SHELXL-97 [62].

Preparation of new nickel(II) complexes

4.1.1. Preparation of $[Ni_2(Msal\text{-}tsc)_2(\mu\text{-}dppm)]$ (1)

3-Methoxysalicylaldehydethiosemicarbazone (0.095 g; 0.420 mmol) was dissolved in dichloromethane (25 cm^3) and this was added to an ethanolic solution of $NiCl_2.6H_2O$ (0.100 g; 0.420 mmol). The mixture was stirred during a clear reddish brown solution was formed. To this 1,1′-bis(diphenylphosphino)methane (0.080 g, 0.210 mmol) was added immediately. After 24 hours stirring, the reaction mixture was filtered and concentrated, whereby a reddish brown solid was obtained. It was washed with petroleum ether (60–80°C) and recrystallized from toluene and methanol to yield reddish brown crystals suitable for X-ray crystallography.

Yield: 53% . M.p. 272 °C. Anal. Calcd for $C_{43}H_{40}N_6O_4S_2Ni_2P_2$: C, 54.48; H, 4.25; N, 8.86; S, 6.76. Found: C, 54.42; H, 4.20; N, 8.79; S, 6.71%. FT-IR (cm^{-1}) in KBr: 1606 ($\nu_{C=N}$), 1305 (ν_{C-O}), 737 (ν_{C-S}); UV-Vis (DMSO), λ_{max}: 263 (93720) nm ($dm^3mol^{-1}cm^{-1}$) (intra-ligand transition); 321(82831) nm ($dm^3mol^{-1}cm^{-1}$) (LMCT s → d); ^{1}H NMR ($CDCl_3$, δ ppm, J Hz): δ 7.835-7.857(d, (J= 8.8), CH=N), δ 6.559- 6.578 (d, (J= 7.6), C4-H), δ 6.419- 6.458 (t, (JH4H5= 7.6), (JH5H6= 8), C5-H), δ 6.677- 6.697 (d, (J= 8), C6-H), δ 4.57 (s, $–NH_2$), δ 3.61 (s,$-OCH_3$), δ 4.108- 4.182 (t, ($–CH_2–$)), δ 7.184- 7.276 & δ 7.912-7.953(m, dppm protons).

The very similar method was followed to synthesize other complexes.

4.1.2. Preparation of $[Ni_2(Msal\text{-}mtsc)_2(\mu\text{-}dppm)]$ (2)

The complex **2** was prepared by the procedure as used for (**1**) with 3-methoxysalicylaldehyde-4(N)-methylthiosemicarbazone [H_2-Msal-mtsc](0.100 g; 0.420 mmol), $NiCl_2.6H_2O$ (0.100 g; 0.420 mmol) and 1,1′-bis(diphenylphosphino)methane (0.080 g, 0.210 mmol).Yield: 51% . M.p: 208 °C. Anal. Calcd for $C_{45}H_{44}N_6O_4S_2Ni_2P_2$: C, 55.37; H, 4.54; N, 8.61; S, 6.57. Found: C, 55.33; H, 4.51; N, 8.58; S, 6.52%. FT-IR (cm^{-1}) in KBr: 1594 ($\nu_{C=N}$), 1310 (ν_{C-O}), 731 (ν_{C-S}); UV-Vis (DMSO), λ_{max}: 265 (79916) nm ($dm^3mol^{-1}cm^{-1}$) (intra-ligand transition); 313(48072) & 365 (37518) nm ($dm^3mol^{-1}cm^{-1}$) (LMCT s → d); 418 (17261) nm ($dm^3mol^{-1}cm^{-1}$) forbidden (d→d) transition; ^{1}H NMR ($CDCl_3$, δ ppm, J Hz): δ 6.539- 6.562 (dd, (J=1.6, 7.6), C4-H), δ 6.400- 6.438 (t, (JH4H5= 7.6), (JH5H6= 8), C5-H), δ 6.671- 6.695 (dd, (J= 1.6, 8), C6-H), δ 4.529 – 4.542 (d, (J= 5.2), terminal –NH), δ 3.599 (s, $–OCH_3$), δ 2.913- 2.926 (d (J=5.2), $–CH_3$), δ 4.092-4.166 (t, ($–CH_2–$)), δ 7.173- 7.277 & δ 7.911-7.966(m, dppm protons and –CH=N).

4.1.3. Preparation of $[Ni_2(Msal\text{-}etsc)_2(\mu\text{-}dppm)]$ (3)

The complex **3** was prepared by the procedure as used for (**1**) with 3-methoxysalicylaldehyde-4(N)-ethylthiosemicarbazone [H_2-Msal-etsc] (0.106 g; 0.420 mmol), $NiCl_2.6H_2O$ (0.100 g; 0.420 mmol) and 1,1′-bis(diphenylphosphino)methane (0.080 g, 0.210 mmol).Yield: 57%. M.p: 173 °C. Anal. Calcd for $C_{47}H_{48}N_6O_4S_2Ni_2P_2$: C, 56.22; H, 4.81; N, 8.37; S, 6.38. Found: C, 56.18; H, 4.78; N, 8.33; S, 6.34%. FT-IR (cm^{-1}) in KBr: 1611 ($\nu_{C=N}$), 1326 (ν_{C-O}), 738 (ν_{C-S}); UV-Vis (DMSO), λ_{max}: 266 (89502) nm ($dm^3mol^{-1}cm^{-1}$) (intra-ligand transition); 318 (61779) nm ($dm^3mol^{-1}cm^{-1}$) (LMCT s → d); 418 (18500) nm ($dm^3mol^{-1}cm^{-1}$) forbidden (d→d) transition; ^{1}H NMR ($CDCl_3$, δ ppm, J Hz): δ 6.540- 6.559 (d, (J= 7.6), C4-H), δ 6.396- 6.435 (t, (JH4H5= 7.6), (JH5H6= 8), C5-H), δ 6.670- 6.690 (d, (J= 8), C6-H), δ 4.450 (s, terminal –NH), δ 3.599 (s, $–OCH_3$), δ 3.286-3.335 (m, $–CH_2$), δ 1.143-1.179 (t, (J= 7.2), $–CH_3$), δ 4.095-4.169 (t, ($–CH_2–$)), δ 7.171-7.261 & δ 7.892-7.969 (m, dppm protons and –CH=N protons).

4.1.4. Preparation of [Ni_2(Msal-ptsc)$_2$(μ-dppm)] (4)

The complex **4** was prepared by the procedure as used for (**1**) with 3-methoxysalicylaldehyde-4(N)-phenylthiosemicarbazone [H_2-Msal-ptsc] (0.106 g; 0.420 mmol), $NiCl_2.6H_2O$ (0.100 g; 0.420 mmol) and 1,1′-bis(diphenylphosphino)methane (0.080 g, 0.210 mmol).Yield: 63% . M.p: 226 °C. Anal. Calcd for $C_{55}H_{48}N_6O_4S_2Ni_2P_2$: C, 60.05; H, 4.40; N, 7.64; S, 5.83. Found: C, 60.01; H, 4.35; N, 7.59; S, 5.78 %. FT-IR (cm^{-1}) in KBr: 1592 ($\nu_{C=N}$), 1315 (ν_{C-O}), 732 (ν_{C-S}); UV-Vis (DMSO), λ_{max}: 268 (51668) nm ($dm^3mol^{-1}cm^{-1}$) (intra-ligand transition); 327 (34652) &371 (25668) nm ($dm^3mol^{-1}cm^{-1}$) (LMCT s → d); 429 (13729) nm ($dm^3mol^{-1}cm^{-1}$) forbidden (d→d) transition; ^{1}H NMR ($CDCl_3$, δ ppm, J Hz): δ 8.122- 8.144 (d, (J=8.8), CH=N), δ 6.589- 6.605 (d, (J= 6.4), C4-H), δ 6.449- 6.488 (t, (JH4H5= 7.6), (JH5H6= 8), C5-H), δ 6.743- 6.763 (d, (J= 8), C6-H), δ 7.495-7.518 (d, (J= 9.2), $C_{2'}$-H & $C_{6'}$-H), δ 7.941-7.986 (t, (J (H6'H5') =8.4, J(H2'H3') =9.6), $C_{3'}$-H & $C_{5'}$-H), δ 6.944-6.995 (m, ($C_{4'}$-H), δ 5.29 (s, terminal –NH), δ 3.631 (s, $–OCH_3$), δ 4.159-4.232 (t, ($–CH_2–$)), δ 7.192-7.473 (m, dppm protons).

4.2. DNA binding study

All of the experiments involving the binding of the compounds with CT DNA were carried out in deionised water with tris(hydroxymethyl)-aminomethane (Tris, 5 mM) and sodium chloride (50 mM) and adjusted to pH 7.2 with hydrochloric acid at room temperature. The concentration of CT-DNA was determined by absorption spectroscopy, using the molar absorption coefficient (6600 $M^{-1}cm^{-1}$) at 260 nm. A stock solution of CT-DNA was stored at

277 K and used after no more than 4 days. The complexes were dissolved in minimum amount of DMSO and diluted with deionized water to the required concentrations prior to use (1% DMSO (v/v) in the final solution). The absorption titrations of the Ni(II) complexes were done using a fixed concentrations of the the Ni(II) complexes (10μM) with varying concentration of CT-DNA (5-50μM). While measuring the absorption spectra, an equal concentration solution of CT-DNA was added to both the nickel complex solution and the reference solution to eliminate the absorbance of CT-DNA itself. Control experiments with DMSO were performed and no changes in the spectra of CT-DNA were observed. The magnitude of the binding strength of the compounds with CT-DNA can be estimated through the binding constant K_b, which can be obtained by monitoring the changes in the absorbance of the corresponding λ_{max} with increasing concentrations of CT-DNA and is given by the (eqn (3)) [63,64].

$$[DNA]/[\varepsilon_a-\varepsilon_f]) = [DNA]/[\varepsilon_b-\varepsilon_f]+1/K_b[\varepsilon_b-\varepsilon_f] \quad (3)$$

The absorption coefficients ε_a , ε_f and ε_b correspond to A_{obsd} / [DNA], the extinction coefficient for the free complex and the extinction coefficient for the complex in the fully bound form respectively. The slope and the intercept of the linear fit of the plot of $[DNA]/[\varepsilon_a - \varepsilon_f]$ versus [DNA] give $1/[\varepsilon_a-\varepsilon_f]$ and $1/K_b[\varepsilon_b-\varepsilon_f]$, respectively. The intrinsic binding constant K_b can be obtained from the ratio of the slope to the intercept [63].

Luminescence titration in the presence of ethidium bromide (EB)

The competitive interactions of each of the complexes **1–4** with EB have been investigated by fluorescence spectroscopy in order to inspect whether the compound can displace EB from its DNA–EB complex. EB fluorescence displacement experiments were conducted by adding the solution of the complexes to the Tris-HCl buffer of a DNA–EB mixture. Before measurements, the mixture was shaken up and recorded. The fluorescence spectra of DNA bound EB were obtained in the excitation (λex) and emission (λem) wavelengths of 515 and 602 nm, respectively. Luminescence titration quenching experiments were conducted by keeping the constant concentration of DNA in buffer-EB (10 μM) with the various concentrations (10-100 μM) of Ni(II) complex solutions. Control experiments with DMSO were performed and no changes in the spectra of DNA-EB were observed. The Stern–Volmer constant K_{SV} is used to evaluate the quenching efficiency of each complex.

4.3. Bovine serum albumin binding study

Binding of the test commplexes (**1-4**) with bovine serum albumin (BSA) was studied using fluorescence spectra recorded with an excitation at 280 nm and corresponding emission at 346 nm assignable to that of free bovine serum albumin (BSA). The excitation and emission slit widths and scan rates were maintained constant for all the experiments. Stock solution of BSA was prepared in 50 mM phosphate buffer (pH=7.2) and stored in the dark at 4°C for further use. Concentrated stock solution of complexess were prepared by dissolving the compounds in DMSO and diluted suitably with deionised water to required concentrations for all the experiments (1% DMSO (v/v) in the final solution). Titrations were manually done by using micropipette for the addition of compounds. Control experiments with DMSO were performed and no changes in the spectra of DNA-EB were observed. For synchronous fluorescence spectra also, the same concentration of BSA and compounds were used and the spectra were measured at two different $\Delta\lambda$ (difference between the excitation and emission wavelengths of BSA) values such as 15 and 60 nm [43].

4.4 Evaluation of antioxidant activity

4.4.1 DPPH (1,1-diphenyl-2-picryl-hydrazyl) radical scavenging assay

The potential antioxidant activity of the compounds were evaluated by DPPH radical-scavenging assay by using the method of Szabo [65]. DPPH free radicals are used for rapid analysis of antioxidants.While scavenging the free radicals, the antioxidants donate hydrogen and form a stable DPPH-H molecule. Briefly, the various concentrations of the complexes (20-100 µg/ml) in 1 ml of 10% DMSO were added to 5 ml of DPPH (0.1 mM in methanol) and were mixed rapidly. Radical scavenging capacity was measured at 10 min intervals using spectrophotometer by monitoring the decrease in absorbance at 517 nm. The IC_{50} values of DPPH decolonization of the complexes were calculated. Ascorbic acid was used as a positive control.

4.4.2 Reductive ability

Total reducing power was determined as described by Oyaizu [66]. The various concentrations(20-100 µg/ml) of the complexes in 1 ml of 10% DMSO were mixed with 2.5 ml of phosphate buffer (0.2 mol/l, pH 6.6) and 2.5 ml of potassium ferricyanide (1%). The mixture was incubated at 50 ºC for 20 min. To this mixture 2.5 mL of 10% trichloro-acetic acid was added and the mixture was centrifuged at 3000 rpm for 20 min. The upper layer (2.5 mL) was mixed with 2.5 mL of deionised water and 0.5 mL of 0.1% ferric chloride and the

absorbance was measured at 700 nm using a spectrophotometer. Increased absorbance of the reaction mixture indicated increased reducing power.

4.4.3 Superoxide anion scavenging activity

Measurement of superoxide anion scavenging activity of the new nickel(II) complexes were done based on the method described by Liu [67]. Super oxide radicals were generated in PMS-NADH systems by oxidation of NADH and assayed by the reduction of nitroblue tetrazolium (NBT). 3 ml of sample solutions at different concentrations (20-100 µg/ml) were mixed with 1 ml of NBT (156 µM) and 1 ml of NADH (468 µM). The reaction was initiated by adding 0.1 ml of phenazine metho sulphate (PMS) solution (60 µM) to the mixture. The reaction was incubated at 25 ºC for 5 min, and the absorbance at 560 nm was measured against blank. Decreased absorbance of the reaction mixture indicates increased super oxide anion scavenging activity. Butylated hydroxy toluene (BHT) was used as the standard.

4.4.4 Estimation of Total antioxidant capacity

Total antioxidant was determined by phosphomolybdenum method [68] followed by Samples and standard (1ml) was mixed with 2 ml of reagent solution [ammonium molybdate (4 mM), sodium phosphate (28 mM) and sulphuric acid (0.6 M)]. All the reaction mixtures were incubated at 95 ºC for 90 min. The absorbance was measured at 695 nm. Total antioxidant activity was expressed as the number of equivalent of ascorbic acid (µg/ml AA).

For the above four assays, all the tests were run in triplicate and various concentrations of the complexes were used to fix a concentration at which complexes showed in and around 50 % of activity. In addition, the percentage of activity was calculated using the formula, % of activity=$[(A_0 - A_C)/A_0] \times 100$. A_0 and A_C are the absorbance in the absence and presence of the tested complex respectively. The IC_{50} (half maximal inhibitory concentration) is a measure of the effectiveness of the substance in inhibiting a specific biological or biochemical function. The 50 % of activity (IC_{50}) can be calculated using the percentage of activity results. All experimental results were expressed as the mean and (±) standard deviation (SD) of triplicate determinations.

4.5 Cytotoxic studies

Cell-culture

Human lung adenocarcinoma cells, A549 were obtained from NCCS, Pune, India. Cells were grown in DMEM and 10% FBS (v/v), containing 100 units/ml penicillin, 30 mg/ml streptomycin and 20mg/ml gentamicin in a CO2incubator with 5% CO_2.

Cell proliferation (MTT) assay

Effect of the complexes on the viability of human lung cancer cells (A549) was assayed by the 3-(4,5-dimethylthiazol-2-yl)-2,5-diphenyltetrazolium bromide (MTT) assay [69]. The cells were seeded at a density of 10,000 cells per well, in 200 µl DMEM medium and were allowed to attach overnight in a CO_2 incubator. Then flick off the media and the complexes (**1-4**) dissolved in 10% DMSO and diluted in cell culture media were added to the cells at a final concentration of 1, 10, 25 and 50 µM. Triplicate was maintained and the medium containing without the compounds were served as control. After 48 h, the wells were treated with 20µl MTT (5 mg/ml PBS) and incubated at 37 °C for 4 h. The purple formazon crystals formed were dissolved in 200µl DMSO and read at 570 nm in a micro plate reader. The mean absorbance for each drug dose was expressed as a percentage of the untreated control well absorbance and was plotted vs. drug concentration. IC_{50} values represent the drug concentrations that reduced the mean absorbance at 570 nm to 50% of those in the untreated control wells and a graph was plotted with the percentage of cell inhibition versus concentration. From this, the IC_{50} value was calculated.

% inhibition = [mean OD of untreated cells(control)/mean OD of treated cells (control)]×100

ACKNOWLEDGEMENT

Department of Science and Technology (SR/FT/CS-32-/2011 dated 04.05.2012) and **Council of Science and Industrial Research** (01(2553)/12/EMR-II dated 03.04.2012) **New Delhi, India** are greatly acknowledged for their financial support. The author G.K. greatly acknowledged **DST, New Delhi, India** for INSPIRE fellowship (IF140225 dated 23.01.2014). The author A.S. greatly acknowledged **UGC, New Delhi, India** for UGC-BSR fellowship (F.25-1/2013-14(BSR)/7-26/2007(BSR)dated 30.05.2014).

Supporting information

Crystallographic data for the complexes **1** and **3** have been deposited at the Cambridge Crystallographic centre as supplementary publication (CCDC No.1443219 and

CCDC No. 1443220). The data can be obtained free of charge at w.w.w.ccdc.cam.ac.uk/conts/retrieving.html/

REFERENCES:

[1] I. Papanastasiou, A. Tsotinis, N. Kolocouris, S.R. Prathalingam, J.M. Kelly, Design, synthesis, and trypanocidal activity of new aminoadamantane derivatives, J. Med. Chem. 51 (2008) 1496-1500.

[2] D. Sriram, P. Yogeeswari, R. Thirumurugan, R.K. Pavana, Discovery of New Antitubercular Oxazolyl Thiosemicarbazones, J. Med.Chem. 49 (2006) 3448-3450.

[3] J.P. Scovill, D.L. Klayman, D.G. Franchino, 2-Acetylpyridine thiosemicarbazones. 4. Complexes with transition metals as antimalarial and antileukemic agents, J. Med. Chem. 25 (1982) 1261-1264.

[4] H. Huang, Q. Chen, X. Ku, L. Meng, L. Lin, X. Wang, C. Zhu, Y. Wang, Z. Chen, M. Li, H. Jiang, K. Chen, J. Ding, H. Liu, A series of alpha-heterocyclic carboxaldehyde thiosemicarbazones inhibit topoisomerase II alpha catalytic activity, J. Med. Chem. 53 (2010) 3048-3064.

[5] M.D. Hall, N.K. Salam, J.L. Hellawell, H.M. Fales, C.B. Kensler, J.A. Ludwig, G. Szakacs, D.E. Hibbs, M.M. Gottesman, Synthesis, Activity, and Pharmacophore Development for Isatin-β-thiosemicarbazones with Selective Activity toward Multidrug-Resistant Cells, J. Med. Chem. 52 (2009) 3191−3204.

[6] M.D. Hall, K.R. Brimacombe, M.S. Varonka, K.M. Pluchino, J.K. Monda, J. Li, M.J. Walsh, M.B. Boxer, T.H. Warren, H.M. Fales, M.M. Gottesman, Synthesis and Structure–Activity Evaluation of Isatin-β-thiosemicarbazones with Improved Selective Activity toward Multidrug-Resistant Cells Expressing P-Glycoprotein, J. Med. Chem. 54 (2011) 5878−5889.

[7] S. Adsule, V. Barve, D. Chen, F. Ahmed, Q.P. Dou, S. Padhye, F.H. Sarkar, Novel Schiff Base Copper Complexes of Quinoline-2 Carboxaldehyde as Proteasome Inhibitors in Human Prostate Cancer Cells, J. Med. Chem. 49 (2006) 7242−7246.

[8] D.R. Richardson, D.S. Kalinowski, V. Richardson, P.C. Sharpe, D.B. Lovejoy, M. Islam, P.V. Bernhardt, 2-Acetylpyridine Thiosemicarbazones are Potent Iron Chelators and Antiproliferative Agents: Redox Activity, Iron Complexation and Characterization of their Antitumor Activity, J. Med. Chem. 52 (2009) 1459−1470.

[9] N. Farrell, Biomedical uses and applications of inorganic chemistry, An overview, Coord. Chem. Rev. 232 (2002) 1-4.

[10] S.W. Ragsdale, H.G. Wood, J.A. Morton, L.G. Ljungdahl, D.V. Dervartanian, J.R. Lancaster Jr (Ed.), The Bioinorganic Chemistry of Nickel, VCH, New York, 1988. Chapter 14.

[11] J.G. Tojal, J.L. Pizarro, A.G. Orad, A.R.P. Sanz, M. Ugalde, A.A. Diaz, J.L. Serra, M.I. Arriortua, T. Rojo, Biological activity of complexes derived from thiophene-2-carbaldehyde thiosemicarbazone. Crystal structure of [Ni(C(6)H(6)N(3)S(2))(2)], J. Inorg. Biochem. 86 (2001) 627-633.

[12] M.B. Ferrari, F. Bisceglie, G. Pelosi, P. Tarasconi, R. Albertini, A. Bonati, P. Lunghi, S. Pinelli, Synthesis, characterisation, X-ray structure and biological activity of three new 5-formyluracil thiosemicarbazone complexes, J. Inorg. Biochem. 83 (2001) 169-179.

[13] M.B. Ferrari, F. Bisceglie, G. Pelosi, P. Tarasconi, R. Albertini, P.P. Dall'Aglio, S. Pinelli, A. Pergamo, G. Sava, Synthesis, characterization and biological activity of copper complexes with pyridoxal thiosemicarbazone derivatives. X-ray crystal structure of three dimeric complexes, J. Inorg. Biochem. 98 (2004) 301-312.

[14] A. Ali, A.H. Mirza, A.M.S. Hossain, M. Nazimuddin, Synthesis, characterization, antifungal properties and X-ray crystal structures of five- and six-coordinate copper(II) complexes of the 6-methyl-2-formylpyridine^{4}N-dimethylthiosemicarbazone, Polyhedron 20 (2001) 1045-1052.

[15] M. Joseph, M. Kuriakose, M.R.P. Kurup, E. Suresh, A. Kishore, S.G. Bhat, Structural, antimicrobial and spectral studies of copper(II) complexes of 2-benzoylpyridine *N*(4)-phenyl thiosemicarbazone, Polyhedron 25 (2006) 61-70.

[16] M.B. Ferrari, C. Pelizzi, G. Pelosi, M.C.R. Arguelles, Preparation, characterization and X-ray structures of 1-methylisatin 3-thiosemicarbazone copper, nickel and cobalt complexes, Polyhedron 21 (2002) 2593-2599.

[17] (a) Applied Homogeneous Catalysis with Organometallic Compounds,ed. B. Cornils and W.A. Herrmann, VCH, New York, 1996, vol. 1, p.2; (b) R. Noyori, Catalysis in Organic Synthesis, John Wiley & Sons, Inc., New York, 1994; (c) G. W. Parshall, S. D. Ittel, Homogeneous Catalysis, John Wiley & Sons, Inc., New York, 2nd edn, 1992, ch. 8; (d) H.B. Kagan, Asymmetric synthesis using organometallic catalysts, in Comprehensive Organometallic Chemistry, ed. G. Wilkinson, F. G. A. Stone and E. W. Abel, Pergamon Press, Oxford, 1982, vol. 8, ch. 53.

[18] (a) F.A. Cotton, B. Hong, Polydentate Phosphines: Their Syntheses, Structural Aspects and Selected Applications, Prog. Inorg. Chem. 40 (1992) 179-289; (b) C. Bianchini, A. Meli, M. Peruzzini, F. Vissa, F. Zanobini, Tripodal polyphosphine ligands

control selectivity of organometallic reactions, Coord. Chem. Rev. 120 (1992) 193-208; (c) D. W. Meek, in Homogeneous Catalysis by Metal Phosphine Complexes, ed. L.H. Pignolet, Plenum, New York, 1983, p. 257; (d) D.W. Meek, D.L. Du Bois, J. Tiethof, Structure and Reactivity Patterns of Polyphosphine Ligands and Their Complexes of Rhodium and Cobalt(I), Adv. Chem. 150 (1976) 335-357.

[19] G.W. Parshall, S.D. Ittel, Homogeneous Catalysis, Wiley, New York, 1992.

[20] F.K. Keter, I.A. Guzei, M. Nell, W.E. Van Zyl, James Darkwa, Phosphinogold(I) Dithiocarbamate Complexes: Effect of the Nature of Phosphine Ligand on Anticancer Properties, Inorg. Chem. 53 (2014) 2058-2067.

[21] A.M. Pyle, J.K. Barton, S.J. Lippard, Probing nucleic acids with transition metal complexes, Prog. Inorg. Chem. 38 (1990) 413-475.

[22] N.A. Kratochwil, M. Zabel, K.J. Range, P.J. Bednarski, Synthesis and X-ray crystal structure of trans, cis-[$Pt(OAc)_2I_2(en)$]: a novel type of cisplatin analogue that can be photolyzed by visible light to DNA-binding and cytotoxic species *in vitro*, J. Med. Chem. 39 (1996) 2499-2507.

[23] T.D. Tullius, Metal–DNA Chemistry, ACS Symposium Series 402, American Chemical Society, Washington DC, 1989.

[24] N. Hadjiliadis and E. Sletten, Metal Complex–DNA Interactions. 2009, Wiley-Blackwell, pp. 133.

[25] A.R. Banerjee, A. Jaeger, D.H. Turner, Thermal Unfolding of a Group I Ribozyme: The Low Temperature Transition is Primarily Disruption of Tertiary Structure, Biochemistry 32 (1993) 153-163.

[26] J. Reedijk, New clues for platinum antitumor chemistry: Kinetically controlled metal binding to DNA, Proc. Natl. Acad. Sci. U. S. A. 100 (2003) 3611-3616.

[27] J. Reedijk, Metal-Ligand Exchange Kinetics in Platinum and Ruthenium complexes, Platinum Met. Rev. 52 (2008) 2-11.

[28] M.D. Hall, M. Okabe, D.W. Shen, X.J. Liang, M.M. Gottesman, The role of cellular accumulation in determining sensitivity to platinum-based chemotherapy, Annu. Rev. Pharmacol. 48 (2008) 495-535.

[29] X. Gao, X. Wang, J. Ding, L. Lin, Y. Li, Z. Guo, Antitumor active monofunctional platinum (II) complexes: Synthesis, structural characterization and reactivity towards biomolecules, Inorg. Chem. Commun. 9 (2006) 722-726.

[30] F. Huq, J. Qing Yu, H. Daghriri, P. Beale, Studies on activities, cell uptake and DNA binding of four trans-planaramine-platinum(II) complexes of the form: trans-$PtL(NH_3)Cl_2$

where L=2- hydroxypyridine, imidazole, 3-hydroxypyridine and imidazo(1,2- α)pyridine, J. Inorg. Biochem. 98 (2004) 1261-1270.

[31] H. Tayyem, F. Huq, J.Q. Yu, P. Beale, K. Fisher, Synthesis and activity of a trinuclear platinum complex: [{trans-$PtCl(NH_3)_2$}$_2$ -{trans-Pt(3-hydroxypyridine)$_2$($H_2N(CH_2)_6NH_2)_2$}]Cl_4 in ovarian cancer cell lines, Chem. Med. Chem. 3 (2008) 145-151.

[32] V.S. Li, D. Choi, Z. Wang, L.S. Jimenez, M.S. Tang and H. Kohn, Role of the C-10 Substituent in Mitomycin C-1-DNA Bonding, J. Am. Chem. Soc. 118 (1996) 2326-2331.

[33] G. Zuber, J.C. Quada and S.M. Hecht, Sequence selective cleavage of a DNA octanucleotide by chlorinated bithiazoles and bleomycins, J. Am. Chem. Soc. 120 (1998) 9368-9369.

[34] A. Atkinson, D.R. Winge, Metal acquisition and availability in the mitochondria, Chem. Rev. 109 (2009) 4708-4721.

[35] B.P. Esposito, R. Najjar, Interactions of antitumoral platinum-group matallodrugs with albumin, Coord. Chem. Rev. 232 (2002) 137-149.

[36] K.B. Beckman, B.N. Ames, The free radical theory of aging matures, Phys. Rev. 78 (1998) 547-581.

[37] B. Halliwel, J.M.C. Gutteridge, Clarendon Press, Oxford, 1989, 494.

[38] G. Pelosi, F. Bisceglie, F. Bignami, P. Ronzi, P. Schiavone, M. Carla Re, C. Casoli, E. Pilotti, Antiretroviral Activity of Thiosemicarbazone Metal Complexes, J. Med. Chem. 53 (2010) 8765-8769.

[39] M. Frezza, S.S. Hindo, D. Tomco, M.M. Allard, Q.C. Cui, M.J. Heeg, D. Chen, Q.P. Dou, C.N. Verani, Comparative Activities of Nickel(II) and Zinc(II) Complexes of Asymmetric [NN'O] Ligands as 26S Proteasome Inhibitors, Inorg. Chem. 48 (2009) 5928-5937.

[40] T. Chattopadhyay, M. Mukherjee, A. Mondal, P. Maiti, A. Banerjee, K.S. Banu, S. Bhattacharya, B. Roy, D.J. Chattopadhyay, T.K. Mondal, M. Nethaji, E. Zangrando and D. Das, A Unique Nickel System having Versatile Catalytic Activity of Biological Significance, Inorg. Chem. 49 (2010) 3121-3129.

[41] P. Kalaivani, R. Prabhakaran, E. Ramachandran, F. Dallemer, G. Paramaguru, R. Renganathan, P. Poornima, V. Vijaya Padma, K. Natarajan, Influence of terminal substitution on structural, DNA, protein binding, anticancer and antibacterial activities of palladium (II) complexes containing 3-methoxy salicylaldehyde-4 (N) substituted thiosemicarbazones, Dalton Trans. 41 (2012) 2486-2499.

[42] S. Priyarega, P. Kalaivani, R. Prabhakaran, T. Hashimoto, A. Endo, K. Natarajan, Nickel(II) complexes containing thiosemicarbazone and triphenylphosphine: Synthesis, spectroscopy, crystallography and catalytic activity, J. Mol. Stuct. 1002 (2011) 58-62.

[43] P. Kalaivani, S. Saranya, P. Poornima, R. Prabhakaran, F. Dallemer, V. Vijaya Padma, K. Natarajan, Biological evaluation of new nickel(II) metallates: Synthesis, DNA /protein binding and mitochondrial mediated apoptosis in human lung cancer cells (A549) via ROS hypergeneration and depletion of cellular antioxidant pool, Eur. J. Med. Chem. 82 (2014) 584-599.

[44] M.L. Torres, A. Fernandez, J.J. Fernandez, A. Suarez, S.C. Juiz, T. Pereira, J. M. Vila, Polynuclear cyclometallated palladium(II) complexes. Crystal and molecular structures of [(PPh$_3$)(Cl)PdN(Cy)□C(H)C$_6$H$_2$C(H)□N(Cy) Pd(Cl)(PPh$_3$)] and [{PdN(Cy)□C(H)C$_6$H$_2$C(H)□N(Cy)Pd}{Ph$_2$PC(H)□C(H)PPh$_2$-*P*,*P*}$_2$][ClO$_4$]$_2$, J. Org. Mett. Chem. 655 (2002) 127-133.

[45] R. Prabhakaran, P. Kalaivani, P. Poornima, F. Dallemer, G. Paramaguru, V. Vijaya Padma, R. Renganathan, R. Huang, K. Natarajan, One pot synthesis of structurally different mono and dimeric Ni(II) thiosemicarbazone complexes and N-arylation on a coordinated ligand: a comparative biological study, Dalton Trans. 41 (2012) 9323-9336.

[46] P. Kalaivani, R. Prabhakaran, F. Dallemer, P. Poornima, E. Ramachandran, E. Vaishnavi, V. Vijaya Padma, R. Renganathan, K. Natarajan, DNA, protein binding, cytotoxicity, cellular uptake and antibacterial activities of new palladium(II) complexes of thiosemicarbazone ligands: effects of substitution on biological activity, Metallomics. 4 (2012) 101-113.

[47] P.T. Selvi , H.S. Evans, M. Palanaindavar, Synthesis, structure and DNA interaction of cobalt(III)bis-complexes of 1,3-bis(2-pyridylimino)isoindoline and 1,4,7-triazacyclononane, J. Inorg. Biochem. 99 (2005) 2110-2118.

[48] M. Chauhan, F. Arimand, K. Banerjee, DNA Binding Studies of Novel Copper(II) Complexes Containing L-Tryptophan as Chiral Auxiliary: In Vitro Antitumor Activity of Cu−Sn$_2$Complex in Human Neuroblastoma Cells, Inorg. Chem. 46 (2007) 3072-3082.

[49] Y.Z. Zhang, H.R. Li, J. Dai, W.J. Chen, J. Zhang, Y. Liu, Spectroscopic studies on the binding of cobalt(II) 1,10-phenanthroline complex to bovine serum albumin, Biol. Trace. Elem. Res. 135 (2010) 136-152.

[50] H.Y. Liu, Z.H. Xu, X.H. Liu, P.X. Xi, Z.Z. Zeng, Analysis of binding interaction between bovine serum albumin and the cobalt(II) complex with salicylaldehyde-2-phenylquinoline-4-carboylhydrazone, Chem. Pharm. Bull. 57 (2009) 1237-1242.

[51] M. Jiang, M.X. Xie, D. Zheng, Y. Liu, X.Y. Li, X. Chen, Spectroscopic studies on the interaction of cinnamic acid and its hydroxyl derivatives with human serum albumin. Journal of Molecular Structure, J. Mol. Struct. 692 (2004) 71-80.

[52] N. Wang, L. Ye, B.Q. Zhao, J.X. Yu, Spectroscopic studies on the interaction of efonidipine with bovine serum albumin, J. Med. Biol. Res. 41 (2008) 589-595.

[53] M.S. Blois, Antioxidant Determinations by the Use of a Stable Free Radical, Nature. 26 (1958) 1199-1200.

[54] R. Singh, S. Singh, S. Kumar and S. Arora, Free radical-scavenging activity of actone extract/fractions of Acacia auriculiformis A. Cunn, Food. Chem. 103 (2007) 1403–1410.

[55] G. Psomas, P. Kessissoglou, Quinolones and non-steroidal anti-inflammatory drugs interacting with copper(II), nickel(II), cobalt(II) and zinc(II): structural features, biological evaluation and perspectives, Dalton. Trans., 2013, **42**, 6252-6276**.**

[56] K.C. Skyrianou, F. Perdih, A.N. Papadopoulos, I. Turel, D.P. Kessissoglou and G. Psomas, Nickel-quinolones interaction Part 5-Biological evaluation of nickel(II) complexes with first-, second- and third-generation quinolones, J. Inorg. Biochem. 105 (2011) 1273-1285.

[57] Y. Li, Z. Y. Jang and J. Cai Wu, Synthesis, crystal structures, biological activities and fluorescence studies of transition metal complexes with 3-carbaldehyde chromone thiosemicarbazone, Eur. J. Med.Chem. 45 (2010) 5692-5701.

[58] Y. Harinath, D. Harikishore Kumar Reddy, B. Naresh Kumar, Ch. Apparao, K. Seshaiah, Synthesis, spectral characterization and antioxidant activity studies of a bidentate Schiff base, 5-methyl thiophene-2-carboxaldehyde-carbohydrazone and its Cd(II), Cu(II), Ni(II) and Zn(II) complexes, Spectrochim. Act. Part A: Molecular and Biomolecular spectroscopy. 101 (2013) 264-272.

[59] A.I. Vogel, Textbook of Practical Organic Chemistry, 5th ed., Longman, London, 1989, 268.

[60] a) R.H. Blessing, An empirical correction for absorption anisotropy, Acta Crystallogr. Sect. A: Found. Crystallogr. 51 (1995) 33-38; (b) R.H. Blessing, Data reduction and error analysis for accurate single crystal diffraction intensities, Crystallogr. Rev. 1 (1987) 3-58; (c) R.H. Blessing, DREADD – data reduction and eroor analysis for single-crystal diffractometer data, J. Appl. Crystallogr. 22 (1989) 396-397.

[61] G.M. Sheldrick, SHELXTL Version 5.1, An Integrated System for Solving, Refining and Displaying Crystal Structures from Diffraction Data, Siemens Analytical X-ray Instruments, Madison, WI, 1990.

[62] G.M. Sheldrick, SHELXL-97, A Program for Cryst Refinement Release 97-2, Institut fur Anorganische Chemie der Universitat Gottingen, Tammanstrasse 4, D-3400, Gottingen, Germany, 1998.

[63] A. Wolfe, G.H. Shimer, T. Meehan, Polycyclic aromatic hydrocarbons physically intercalate into duplex regions of denatured DNA, Biochemistry 26 (1987) 6392-6396.

[64] G. Cohen, H. Eisenberg, Viscosity and sedimentation study of sonicated DNA–proflavine complexes, Biopolymers 8 (1969) 45-55.

[65] M.R. Szabo, C. Idtoiu, D. Chambre, A.X. Lupea, Improved DPPH determination for antioxidant activity spectrophotometric assay, Chemistry and Materials Science 61 (2007) 214-216.

[66] M. Oyaizu, Studies on product of browning reaction prepared from glucose amine, Jap. J. Nutr. 44 (1986) 307-315.

[67] F. Liu, V.E.C. Ooi, S.T. Chang, Free radical scavenging activities of mushroom polysaccharide extracts, Life Science 60 (1997) 763-771.

[68] P. Prieto, M. Pineda, M. Aguilar, Spectrophotometric quantitation of antioxidant capacity through the formation of a phosphomolybdenum complex: specific application to the determination of Vitamin E, Analytical Biochemistry 269 (1999) 337-341.

[69] T. Mossman, Rapid colorimetric assay for cellular growth and survival: application to proliferation and cytotoxicity assays, J. Immunol. Methods 65 (1983) 55-63.

DNA(CT), Protein(BSA) binding studies, anti-oxidant and cytotoxicity studies of new binuclear Ni(II) complexes containing 4(N)- substituted thiosemicarbazones

G. Kalaiarasi,[a] C. Umadevi,[a] A. Shanmugapriya,[a] P. Kalaivani,[b] F. Dallemer [c] and R. Prabhakaran [a*]

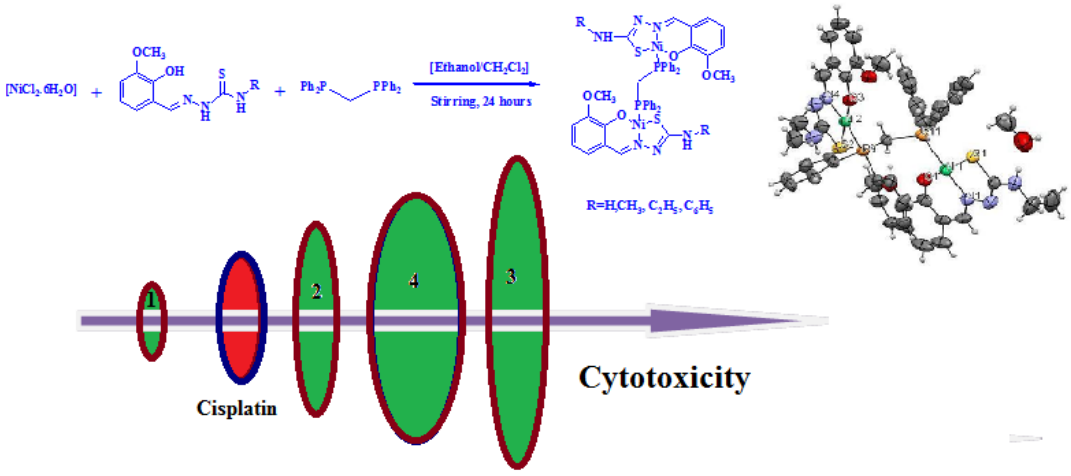

Potential biological properties (CT-DNA binding, BSA-protein binding, anti- oxidant and cytotoxicity) of new N-substituted thiosemicarbazone Nickel(II) complexes have been investigated

HIGHLIGHTS

- Four new binuclear nickel(II) complexes have been synthesized and characterized
- The DNA and protein interactions of these complexes were studied by a variety of techniques. It binds to CT-DNA via intercalation, and its strongly bind with albumin protein
- Nickel complexes exhibited significant in vitro antioxidant activity.
- The cytotoxic activity was evaluated against a human lung cancer cell line A549
- The complexes (**2** (IC_{50}=23 µM)**, 3** (IC_{50}=12 µM) & **4** (IC_{50}=20 µM)) exhibited a good anticancer activity over the standard drug, *Cisplatin* (IC_{50}=25 µM)